Metallophysics and Advanced Technologies
Металофіз. новітні технол.
Metallofiz. Noveishie Tekhnol.
2022, vol. 44, No. 9, pp. 1147–1161
https://doi.org/10.15407/mfint.44.09.1147
Reprints available directly from the publisher

PACS numbers: 43.35.Cg, 62.20.Dc, 63.20.Kr

Elastic, Mechanical and Thermophysical Properties of Hexagonal Nanostructured Cr_2N Compound

Aadesh K. Prajapati[*], Navin Chaurasiya[*,**], Sachin Rai[*], and Pramod K. Yadawa[*]

[*]*Department of Physics, Institute of Physical Sciences for Study and Research, V. B. S. Purvanchal University, 222003 Jaunpur, India*
[**]*Department of Mechanical Engineering, UNSIET, V. B. S. Purvanchal University, 222003 Jaunpur, India*

The characteristic features of hexagonally Cr_2N compound is considered by the theoretical valuation of elastic, mechanical, ultrasonic and thermophysical properties. Initially, the higher order elastic constants (HOECs) of nanostructured Cr_2N material are computed using the Lennard-Jones many body interactions potential approach. With the help of the HOECs such as modulus like Young's, bulk and anisotropic parameters are evaluated for elastic and mechanical characterization. Temperature dependent ultrasonic velocities, Debye average velocity and thermal relaxation time are also evaluated along orientation dependent. The ultrasonic attenuation (UA) of longitudinal and shear wave due to phonon–phonon (p–p) interaction and thermoelastic relaxation mechanism are investigated for this thin film. The thermal conductivity is a principal contributor to the behaviour of UA due to p–p interactions. Mechanical and thermal properties of the nanostructured Cr_2N are superior at low temperature.

Key words: novel hard chromium-based materials, nanostructured compound, thermal conductivity, elastic properties, ultrasonic properties.

Розглянуто характерні особливості гексагональної сполуки Cr_2N шляхом теоретичної оцінки пружних, механічних, ультразвукових і теплофізич-

Corresponding author: Pramod K. Yadawa
E-mail: pkyadawa@gmail.com

Citation: Aadesh K. Prajapati, Navin Chaurasiya, Sachin Rai, and Pramod K. Yadawa, Elastic, Mechanical and Thermophysical Properties of Hexagonal Nanostructured Cr_2N Compound, *Metallofiz. Noveishie Tekhnol.*, **44**, No. 9: 1147–1161 (2022). DOI: 10.15407/mfint.44.09.1147

них властивостей. Було обчислено пружні константи вищих порядків (ПКВП) наноструктурованого матеріялу Cr_2N з використанням багаточастинкового потенціялу Леннард-Джонса. За допомогою обчислених ПКВП, а саме модуля Юнґа, об'ємних та анізотропних параметрів, було оцінено пружні і механічні характеристики. Залежні від температури швидкості ультразвуку, середня швидкість Дебая та час теплової релаксації також були оцінені для різних орієнтацій. Було досліджено ультразвукове загасання (УЗ) поздовжньої та зсувної хвиль внаслідок фонон-фононної взаємодії та механізм термопружної релаксації. Теплопровідність є основним чинником, що впливає на поведінку УЗ за рахунок фонон-фононної взаємодії. Механічні та термічні властивості наноструктурованого Cr_2N покращуються при пониженні температури.

Ключові слова: міцні матеріяли на основі хрому, наноструктурована сполука, теплопровідність, пружні властивості, ультразвукові властивості.

(Received December 05, 2021; in final version, August 4, 2022)

1. INTRODUCTION

CrN (chromium nitride) has a rigid and wear-resistant, semiconductor composite. It was achieved concern for numerous applications such as medicinal implants [1]. CrN is an alluring thin film material as a result of his refractory character and mechanical properties. It was utilized as a defensive layered material due to his high hardness, high melting point, good thermal conductivity and greater corrosion resistance. The thin film of CrN is existing in cubic structure (CrN) and hexagonal structure (Cr_2N) phases, therefore its characteristics are depending on crystalline phase [2]. In peculiar the evolution of crystalline phases mostly depends on deposition conditions [3]. Cr_2N is a significant member of Cr–N composites that shows more properties [4–6]. It has stimulating thermal and thermoelectric properties [7]. Surface morphology that can transform thin film properties show a significant character in applications, like as metallization and wear-resistant coatings [8]. CrN thin films exhibition semiconductor properties [9] with a band gap of 0.7 eV [10], exceptional spectral selectivity and extremely small emission, and consequently can be utilized for solar selective absorbent material [11]. Various experimental studied shown different consequences on the electron carriage properties of CrN materials. Consequently, it remains static an exposed concern in the material thereby associated structural and electronic phase transformation [12].

Ultrasonic attenuation (UA) is the exact main physical parameter to describe a material, whichever appreciates the specific relationship between the anisotropic behaviour of proximal hematinic planes and the affinity and structural motion, some physical measures like ther-

mal energy density, specific heat and thermal conductivity, is well associated with higher-order elastic constants [13].

In this work, we were worked diligently to make the relationship between thermo physical and microstructural properties for nanostructured Cr_2N compound will help in understanding the mechanical behaviour of nanostructured thin film, which size is 30 nm and it will performance and significant role in the diagram of manufacturing apparatus with useful physical properties under moderate working conditions. For that, we have considered acoustic coupling constants, ultrasonic attenuation coefficient, elastic stiffness constant, thermal relaxation time and the ultrasonic velocity since nanostructured Cr_2N film. The shear modulus (G), bulk modulus (B), Young's modulus (Y), Poisson's ratio, Pugh's ratio (B/G) and anisotropic parameters were also calculated and discussed for nanostructured Cr_2N material.

2. THEORY

In present work, the Lennard-Jones interaction potential model method was using for the evaluation for higher order elastic constants (HOECs). A comprehensive explanation of n^{th} order elastic constant is the part results of the thermodynamic potential to finite deformation as well as mathematically conveyed by subsequent expression as [14, 15]:

$$C_{ijklmn\ldots} = \frac{\partial^n F}{\partial\eta_{ij}\partial\eta_{kl}\partial\eta_{mn}\ldots}. \tag{1}$$

Whenever, F is represented free energy density and η_{ij} is represent Lagrangian strain component tensor. Also, F can be extended in relatives of strain η by Taylor series expansion as:

$$F = \sum_{n=0}^{\infty} F_n = \sum_{n=0}^{\infty} \frac{1}{n!} \frac{\partial^n F}{\partial\eta_{ij}\partial\eta_{kl}\partial\eta_{mn}\ldots} \partial\eta_{ij}\partial\eta_{kl}\partial\eta_{mn}\ldots. \tag{2}$$

Thereby, the free energy density is written such as:

$$F_2 + F_3 = \frac{1}{2!} C_{ijkl}\partial\eta_{ij}\partial\eta_{kl} + \frac{1}{3!} C_{ijklmn}\partial\eta_{ij}\partial\eta_{kl}\eta_{mn}. \tag{3}$$

For the h.c.p. compounds, the basis vectors are

$$a_1 = a\left(\frac{\sqrt{3}}{2}, \frac{1}{2}, 0\right),\ a_2 = a(0,1,0),\ a_3 = a(0,0,c)$$

in Cartesian coordinates axes, where a and c represent the unit cell lattice parameters. The unit cell of hexagonal compound contains two

nonequivalent atoms: 6 atoms in basal plane and 3–3 atoms upper and lower the basal plane. The consequently, both first and second neighbourhood contains of six atoms, where

$$r_1 = a(0,0,0),\ r_2 = a\left(\frac{a}{2\sqrt{3}}, \frac{a}{2}, \frac{c}{2}\right)$$

are the position vectors of those two kinds of atoms.

Up to second nearest neighbour, the potential energy per unit cell is scripted following:

$$U_2 + U_3 = \sum_{I=1}^{6} U(r_I) + \sum_{J=1}^{6} U(r_J), \tag{4}$$

where, I refer to atoms in the basal plane and J refers to atoms above and below the basal plane. Whenever the crystal is deformable uniformly then interatomic vectors in non-deformed state **(r)** and deformable state **(r′)** are associated as:

$$(r')^2 - (r)^2 = 2\varepsilon_i \varepsilon_j \eta_{ij} = 2\Theta, \tag{5}$$

whenever, ε_i and ε_j are the Cartesian components of vector **r**. The energy density U may be describing based on Θ as [17, 18]:

$$U_n = (2V_c)^{-1} \sum \frac{1}{n!} \Theta^n D^n \varphi(r)\ . \tag{6}$$

From equations (4) and (6), the energy density U relating cubic terms can be described as:

$$\begin{aligned} U_2 + U_3 = (2V_c)^{-1} \left[\sum_{I=1}^{6} \frac{1}{2!} \Theta_I^2 D^2 \varphi(r_I) + \sum_{J=1}^{6} \frac{1}{2!} \Theta_J^2 D^2 \varphi(r_J) \right] + \\ + (2V_c)^{-1} \left[\sum_{I=1}^{6} \frac{1}{3!} \Theta_I^3 D^3 \varphi(r_I) + \sum_{J=1}^{6} \frac{1}{3!} \Theta_J^3 D^3 \varphi(r_J) \right]. \end{aligned} \tag{7a}$$

Here, $V_c = (3a^2c/2)^{1/2}$ representing the volume of the elementary cell, $D = r^{-1}d/dr$ and $\varphi(r)$ is the interaction potential. The energy density is examined to be function of Lennard-Jones potential and specified as:

$$\varphi(r) = -\frac{a_0}{r^m} + \frac{b_0}{r^n}\ . \tag{7b}$$

Here, a_0, b_0 are represent the coefficients constants, r is the distance between atoms, m, n represent the integer quantity. The interaction potential model leads to six SOECs and ten TOECs of the hexagonal compound and formulations of elastic constants are given as following expressions [14, 15]:

$$
\begin{aligned}
&C_{13} = 1.925\,p^6C', C_{33} = 3.464\,p^8C',\\
&C_{44} = 2.309\,p^4C', C_{66} = 9.851\,p^4C',\\
&C_{111} = 126.9\,p^2B + 8.853\,p^4C', C_{112} = 19.168\,p^2B - 1.61\,p^4,\\
&C_{113} = 1.924\,p^4B + 1.155\,p^6, C_{123} = 1.617\,p^4B - 1.155\,p^6C,\\
&C_{133} = 3.695\,p^6B, C_{155} = 1.539\,p^4B,\\
&C_{144} = 2.309\,p^4B, C_{344} = 3.464\,p^6B,\\
&C_{144} = 101.039\,p^2B + 9.007\,p^4\,C', C_{333} = 5.196\,p^8B,
\end{aligned}
\tag{8}
$$

where $p = c/a$ is axial ratio;

$$
C' = \chi\frac{a}{p^5}, B = \chi\frac{a^3}{3}, \chi = \frac{1}{8}\frac{nb_0(n-m)}{a^{n+4}}, \psi = -\frac{\chi}{6a^2(m+n+6)},
$$

b_0—Lennard-Jones parameter.

The bulk modulus and shear modulus were calculated using Voigt and Reuss methodologies [16, 17]. The calculations of unvarying stress and unvarying strain were used in the Voigt and Reuss methodologies, correspondingly. Furthermore, from Hill's methods, the average values of both methodologies were used toward compute ensuing values of B and G [18]. Young's modulus and Poisson's ratio are considered using values of bulk modulus and shear modulus respectively [19, 20]. The following expressions were used for the evaluation of Y, B, G and σ:

$$
\begin{aligned}
&M = C_{11} + C_{12} + 2C_{33} - 4C_{13}, C^2 = (C_{11} + C_{12})C_{33} - 4C_{13} + C^2,\\
&B_{\mathrm{R}} = \frac{C^2}{M}, \mathrm{B_V} = \frac{2(C_{11} + C_{12}) + 4C_{13} + C_{33}}{9},\\
&G_{\mathrm{V}} = \frac{M + 12(C_{44} + C_{66})}{30}, \mathrm{G_R} = \frac{5C^2C_{44}C_{66}}{2[3B_VC_{44}C_{66} + C^2(C_{44} + C_{66})]},\\
&Y = \frac{9GB}{G + 3B}, \mathrm{B} = \frac{B_{\mathrm{V}} + B_{\mathrm{R}}}{2}, \mathrm{G} = \frac{G_{\mathrm{V}} + G_{\mathrm{R}}}{2}, \sigma = \frac{3B - 2G}{2(3B + G)}.
\end{aligned}
\tag{9}
$$

The anisotropic and mechanical properties of nanostructured materials are well correlated with ultrasonic velocity due to the velocity of ultrasonic wave are mainly depending upon the density and SOECs. As a function of mode of vibration, those are three types of ultrasonic velocities in hexagonal nanostructured compound. First longitudinal V_{L} and second shear (V_{S1}, V_{S2}) waves velocities.

Angle dependent ultrasonic velocities along z axis of the crystal for hexagonal nanostructured materials are specified by following equations:

$$
\begin{aligned}
V_{\mathrm{L}}^2 &= \{C_{33}\cos^2\theta + C_{11}\sin^2\theta + C_{44} + \{[C_{11}\sin^2\theta - C_{33}\cos^2\theta + \\
&+C_{44}(\cos^2\theta - \sin^2\theta)]^2 + 4\cos^2\theta\sin^2\theta(C_{13}+C_{44})^2\}^{1/2}\}/2, \\
V_{S1}^2 &= \{C_{33}\cos^2\theta + C_{11}\sin^2\theta + C_{44} - \{[C_{11}\sin^2\theta - C_{33}\cos^2\theta + \\
&+C_{44}(\cos^2\theta - \sin^2\theta)]^2 + 4\cos^2\theta\sin^2\theta(C_{13}+C_{44})^2\}^{1/2}\}/2\rho, \\
V_{S2}^2 &= \left\{C_{44}\cos^2\theta + C_{66}\sin^2\theta\right\}/\rho.
\end{aligned}
\tag{10}
$$

Here, V_{L}, V_{S1}, and V_{S2} are the longitudinal, quasi-shear and shear wave velocities. Also, ρ is the density of compound and θ is angle with the unique axis of the crystal. The Debye average velocity is specified by the equation as [21, 22]:

$$
V_{\mathrm{D}} = \left[\frac{1}{3}\left(\frac{1}{V_{\mathrm{L}}^3} + \frac{1}{V_{\mathrm{S1}}^3} + \frac{1}{V_{\mathrm{S2}}^3}\right)\right]^{-1/3}. \tag{11}
$$

At this temperature regime, the mean free path of electron is alike as the mean free path of acoustical phonons. Accordingly, a high probability coupling arises between free electrons and acoustic phonons [14]. Ultrasonic attenuation for longitudinal α_{long} and shear waves α_{shear} by the energy loss due to electron-phonon interaction is given by:

$$
\alpha_{\mathrm{long}} = \frac{2\pi^2 f^2}{\rho V_{\mathrm{L}}^3}\left(\frac{4}{3}\eta_e + \chi\right), \tag{12}
$$

$$
\alpha_{\mathrm{shear}} = \frac{2\pi^2 f^2}{\rho V_{\mathrm{S}}^3}\eta_e, \tag{13}
$$

where ρ is the density of nanostructured compound, η_e is the electron viscosity, f is the frequency of the ultrasonic wave and χ is the compression viscosity, V_{L} and V_{S} are the acoustic wave velocities for longitudinal and shear waves respectively and are given as:

$$
V_{\mathrm{L}} = \sqrt{\frac{C_{33}}{\rho}} \text{ and } V_{\mathrm{S}} = \sqrt{\frac{C_{44}}{\rho}}. \tag{14}
$$

The viscosity of the electron gas (η_e) [21, 22] is given by

$$
\eta_e = \frac{9\cdot 10^{11}\hbar^2(3\pi^2 N)^{2/3}}{5e^2 R}. \tag{15}
$$

Here, N is the number of molecules per unit volume, and R is the resistivity.

For p–p interaction (Akhieser's type loss) (at high temperature) and thermoelastic loss, there are the two prevailing processes, whichever

are considerable for attenuation of ultrasonic wave. The attenuation by virtue of Akhieser's loss is specified by following equation:

$$(\alpha / f^2)_{\text{Akh}} = \frac{4\pi^2 \tau E_0 (D / 3)}{2\rho V^3}, \tag{16}$$

where E_0 is the thermal energy density. The acoustical coupling constants D is specified by following expression:

$$D = 3(3E_0 < (\gamma_i^j)^2 > - < \gamma_i^j >^2 C_V T) / E_0. \tag{17}$$

Here C_V represents heat per unit volume of the material, γ_i^j is the Grüneisen number. The time takes for re-establishment of equilibrium of the thermal phonons is called as thermal relaxation time (τ) and is given by:

$$\tau = \tau_{\text{S}} = \tau_{\text{L}} / 2 = \frac{3k}{C_V V_{\text{D}}^2}. \tag{18}$$

Here τ_{L} and τ_{S} represent the thermal relaxation time for the longitudinal wave and shear, k is the thermal conductivity of the nanostructured compound.

The thermoelastic loss $(\alpha/f^2)_{\text{Th}}$ is specified by the following equation [33, 34]:

$$(\alpha / f^2)_{\text{Th}} = 4\pi^2 < \gamma_i^j >^2 \frac{kT}{2\rho V_{\text{L}}^5}. \tag{19}$$

The total ultrasonic attenuation is given by:

$$(\alpha / f^2)_{\text{Total}} = (\alpha / f^2)_{\text{Th}} + (\alpha / f^2)_{\text{L}} + (\alpha / f^2)_{\text{S}}. \tag{20}$$

Here, $(\alpha/f^2)_{\text{Th}}$ represent the thermoelastic loss, $(\alpha/f^2)_{\text{L}}$ and $(\alpha/f^2)_{\text{S}}$ are the coefficients of ultrasonic attenuation for the longitudinal and shear wave, respectively.

3. RESULTS AND DISCUSSION

3.1. Higher-Order Elastic Constants

In current analysis, we have calculated the elastic constants (six SOECs and ten TOECs) using Lennard-Jones potential model. The lattice parameters a and p (axial ratio) for nanostructured Cr_2N compound are 4.752 Å and 0.932 Å respectively [23]. Here, value of b_0 is $1.97 \cdot 10^{-62}$ erg·cm^7 for Cr_2N thin film. Also, the values of m and n for Cr_2N compound are 6 and 7. The values of second order elastic constants (SOECs)

TABLE 1. SOECs and TOECs in GPa at room temperature.

	C_{11}	C_{12}	C_{13}	C_{33}	C_{44}	C_{66}	B
Cr_2N	759	186	53	82	63	297	242

	C_{111}	C_{112}	C_{133}	C_{123}	C_{133}	C_{155}	C_{144}	C_{344}	C_{222}	C_{333}
Cr_2N	−12378	−1962	−135	−171	−278	−260	−200	−133	−9794	−339

and third order elastic constants (TOECs) were calculated for this Cr_2N compound is offered now Table 1.

Nanostructured Cr_2N had the highest elastic constant values, which are important for the material, as these are associated with the stiffness parameter. SOECs are used to determine the UA and associated parameters. Highest elastic constant values found for nanostructured Cr_2N compound are indicative of their better mechanical properties.

Higher-order elastic constants are extents to describe the elasticity of nanomaterials which normalize the response of nanostructured compounds to outward forces. Evidently, for steady of the nanostructured compound, the five independent SOECs (C_{ij}, namely C_{11}, C_{12}, C_{13}, C_{33}, C_{44}) would satisfy the well-known Born–Huang stability norms [19, 20], *i.e.*, $C_{11} - |C_{12}| > 0$, $(C_{11} + C_{12})C_{33} - 2C_{13}^2 > 0$, $C_{11} > 0$ and $C_{44} > 0$, which is understandable since Table 1. It is evident that the values of elastic constant are positive too satisfies Born–Huang mechanical stability constraints and therefore totally this nanostructured thin film is mechanically stable. The bulk modulus for nanostructured Cr_2N thin film can be calculated using Eq. (9) and presented in Table 1. The evaluated value of bulk modulus of nanocrystalline Cr_2N compound is 239.77 GPa, which is same as evaluated by Alexander *et al.* (239.8 GPA) [23]. Thus, there is respectable agreement between the presented and the informed values which is correlated with elastic constants. Therefore, our theoretical methodology is well justified for the evaluation of SOECs of nanostructured compounds. We present the calculated values of TOECs in Table 1. The negative values of TOECs specify a negative strain in the solid. Negative values of TOECs appear in the previous paper on hexagonal structure material. Therefore, the theory applied for evaluation of HOECs is justified [24, 25]. Hence, the applied theory for the valuation of higher order elastic constants is justified.

The values of B, G, Y, B/G and σ for Cr_2N compound at room tem-

TABLE 2. Voigt–Reus constants (M and C^2), B ($\times 10^{10}$ nm^{-2}), G ($\times 10^{10}$ nm^{-2}), Y ($\times 10^{10}$ nm^{-2}), σ, B/G for Cr_2N thin film.

	M	C^2	B_r	B_v	G_r	G_v	Y	B/G	G/B	σ
Cr_2N	817	80087	98	243	88	172	311	1.31	0.76	0.196

TABLE 3. Density ($\rho\times10^3$·kg·m^{-3}), thermal energy density ($E_0\times10^7$ J·m^{-3}), specific heat per unit volume ($C_V\times10^5$ J·m^{-3}·K^{-1}), thermal conductivity ($k\times10^{-5}$·W·m^{-1}·K^{-1}) and the acoustic coupling constant (D_L, D_S) of nanostructured Cr_2N thin film.

	ρ	C_V	E_0	k	D_L	D_S
50 K	6.85	2.17	2.92	0.29	17.36	23.13
100 K	6.80	7.62	2.75	0.47	17.31	23.13
150 K	6.75	10.66	7.31	0.68	17.31	23.13
200 K	6.70	11.92	12.84	0.94	17.32	23.13
250 K	6.65	12.56	18.87	1.27	17.32	23.13
300 K	6.60	12.89	25.08	2.03	17.32	23.13

perature is calculated using eq. (1) and existing in Table 2.

The Cr_2N compound have little stiffness. The ratio of B and G (B/G) and σ are the measure of brittleness and ductility of solid. If the value of $\sigma = 0.196 \leq 0.26$ and $B/G = 1.31 \leq 1.75$, then the solid is generally brittle, otherwise it is ductile in nature [24, 25]. The finding of lower values of B/G and σ compared to their critical values specifies that nanostructured Cr_2N are brittle in nature. For stability of the elastic material, the value of σ should be less than 0.5. Here, value of σ or Cr_2N compound are smaller than its critical value. Thus, it indicates that nanostructured Cr_2N thin film is stable against shear. The hardness, compressibility, ductility, brittleness, toughness and bonding characteristic of the nanostructured material are too well connected with the SOECs.

Elastic anisotropic is an important parameter for mechanical properties of compounds. The elastic anisotropic is well-defined by the following expressions for hexagonal structured compounds [26]: $\Delta P = C_{33}/C_{11}$, where ΔP is the anisotropy for compression waves; $\Delta_{S1} = (C_{11} + C_{13} - 2C_{13})/4C_{44}$, $\Delta_{S2} = 2C_{44}/(C_{11} - C_{12})$. Here, Δ_{S1} and Δ_{S2} rep-

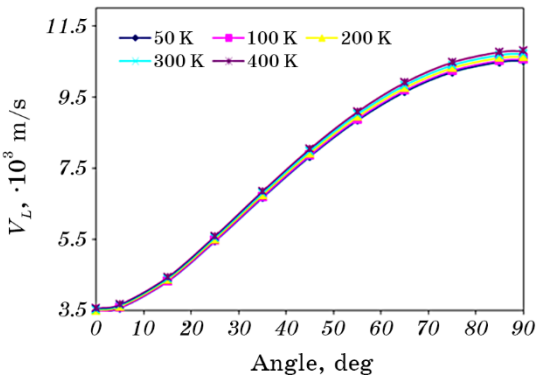

Fig. 1. V_L *vs* angle with *z* axis of crystal.

resent the anisotropy for polarized perpendicular to the basal plane and polarized in the basal plane correspondingly. All these three parameters define the anisotropy of the three main acoustic modes.

The evaluated compression anisotropy of Cr_2N compound is $\Delta P = 0.10$. The value of shear anisotropy Δ_{S1} and Δ_{S2} are 2.91 and 0.22 respectively. The shear anisotropy is large, due to the small values of C_{44}. It shows that the major shear distortion occurs in [100] plane and the error is most possible to occur between planes parallel to [001] plane. For isotropic medium, $\Delta P = \Delta_{S1} = \Delta_{S2} = 1$. Thus, chosen nanostructured Cr_2N is anisotropic. These results designate that the Cr–N bonds are stronger in the layer, which is parallel to the [001] plane than between the layers.

3.2. Ultrasonic Velocity and Allied Constraints

In present analysis, we have correlated the mechanical and isotropic behaviour of the compound with the ultrasonic velocity. We have calculated the longitudinal ultrasonic wave velocity, shear ultrasonic wave velocity, the Debye average velocity and the thermal relaxation time τ for nanostructured Cr_2N compound. The data for the temperature dependent density ρ of nanostructured Cr_2N thin film presented in Table 3 and have been taken from literature [23]. Thermal conductivity k of Cr_2N thin film presented in Table 3 has been taken from the literature [27]. Also, the thermal conductivity of nanostructured Cr_2N thin film has been evaluated from electrical resistivity using Wiedemann–Franz law [28]. The values of temperature dependent specific heat per unit volume (C_V) and thermal energy density (E_0) were calculated using the tables of physical constant and Debye temperatures and acoustic coupling constants (D_L and D_S) are shown in Table 3.

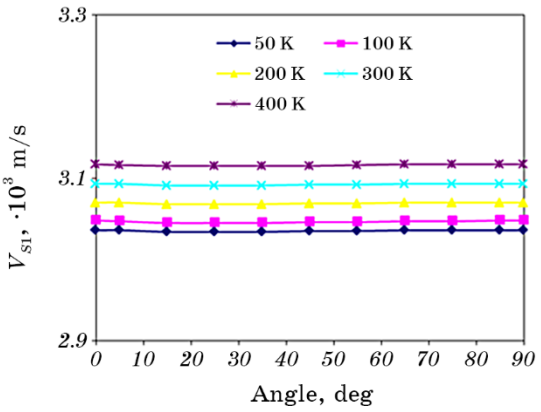

Fig. 2. V_{S1} *vs* angle with *z* axis of crystal.

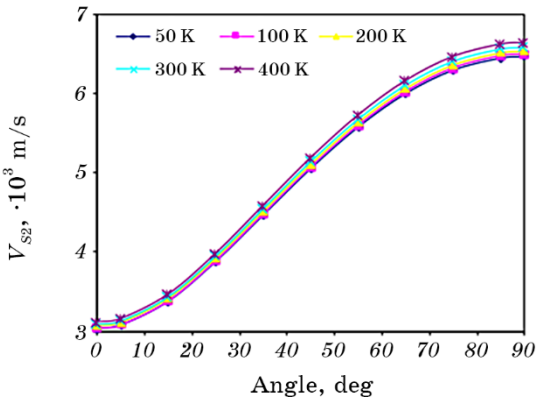

Fig. 3. V_{S2} *vs* angle with *z* axis of crystal.

It is clear form Table 3 that for all temperatures, the values of D_L are smaller than those of D_S for nanostructured Cr_2N thin film. It indicates that for the longitudinal ultrasonic wave the transformation of ultrasonic energy into thermal energy is less than for the shear ultrasonic waves.

The angular dependences of ultrasonic wave velocity (V_L, V_{S1}, V_{S2} and V_D) along *z* axis of the crystal at different temperature are presented in Figs. 1–4. From Figures 1–3, V_L and V_{S2} increases with angle while V_{S1} approximately unchanged with angle form the *z* axis. Abnormal behaviour of angle dependent velocity is due to combined effect of SOECs and density. The nature of the angle dependent velocity curves in the present work is similar to found for other hexagonal-type material [29, 30]. Thus, the angle dependence of the velocities in nanostructured Cr_2N compound is justified.

Figure 4 shows the variation of Debye average velocity (V_D) with the

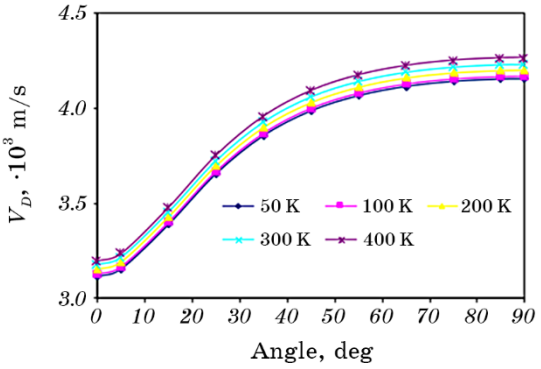

Fig. 4. V_D *vs* angle with *z* axis of crystal.

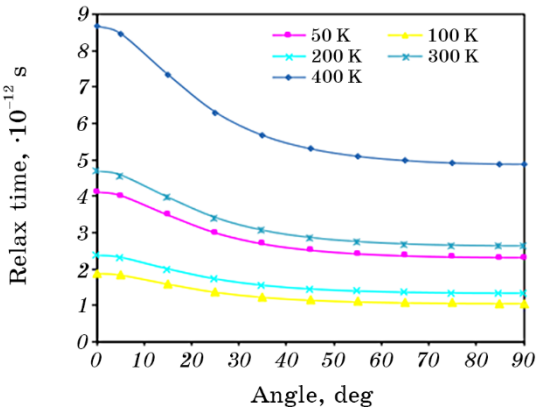

Fig. 5. Relaxation time *vs* angle with *z* axis of crystal.

angle made with the *z* axis of the crystal. It is clear that V_D increases with the angle and reaches maximum at 900 for Cr_2N compound. As the calculation of V_D involves the velocities V_L, V_{S1} and V_{S2} [31, 32]. The variation of V_D is affected by the all three ultrasonic velocities. Maximum value of V_D at 90° is due to a significant increase in longitudinal and shear wave velocities. It may be determined that the average sound wave velocity is a maximum when a sound wave travels at 90° angles with the *z* axis of these crystal.

Figure 5 shows a plot of the calculated thermal relaxation time τ with the angle. The angle dependent thermal relaxation time curves track the reciprocal nature of V_D as $\tau \propto 3K / C_V V_D^2$. Thus, it is clear that thermal relaxation time for hexagonal Cr_2N thin films is mainly affected by the thermal conductivity and thermal energy density. Thermal relaxation time τ is found in order at picoseconds for Cr_2N thin film [29, 33, 34]. Therefore, the evaluated thermal relaxation time explains the nanostructured Cr_2N thin films. The minimum value of τ for wave propagation along $\theta = 90°$ represents that the re-establishment time for equilibrium distribution of thermal phonons will be minimum for propagation of wave along this direction.

3.3. Ultrasonic Attenuation due to p–p-Interaction and Thermal Relaxation Occurrences

For estimating UA, the wave is propagating along the unique axis [<001> direction] of nanostructured Cr_2N thin films. The ultrasonic attenuation coefficient divided by frequency squared $(\alpha/f^2)_{Akh}$ is calculated for the longitudinal wave $(\alpha/f^2)_L$ and for the shear wave $(\alpha/f^2)_S$ using Eq. (16) under the condition $\omega\tau << 1$ at different temperature. Equation (19) has been used to calculate the thermo-elastic loss divided

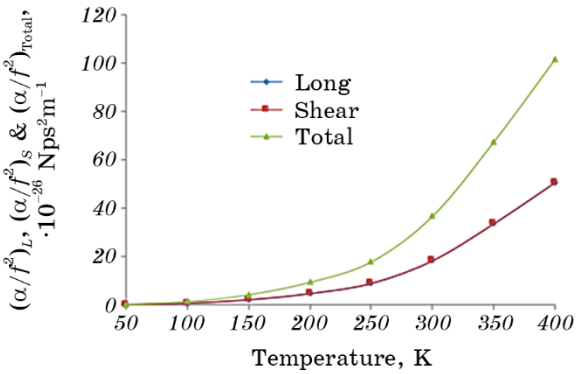

Fig. 6. $(\alpha/f^2)_{Total}$ and $(\alpha/f^2)_{Akh}$ *vs* temperature of Cr_2N thin film.

by frequency squared $(A/f^2)_{Th}$. Figures 6, 7 present the temperature dependent ultrasonic attenuations $(\alpha/f^2)_L$, $(\alpha/f^2)_S$, $(\alpha/f^2)_{Th}$ and total attenuation $(\alpha/f^2)_{Total}$ of Cr_2N thin films.

In this work, the ultrasonic wave is assumed to propagate along the *z* axis of the crystal from Fig. 6. It is evident that the Akhieser type of energy losses for the longitudinal waves, shear waves and the thermoelectric loss increase with temperature of compounds $(\alpha/f^2)_{Akh}$ is proportional to E_0, D, τ and V^{-3}. In Fig. 3 E_0 and V are increasing with temperature. Thus, Akhieser losses in nanostructured Cr_2N thin films are overwhelmingly affected by E_0 and the k.

Consequently, the increase in UA is due to the increase in thermal conductivity. Therefore, it is the p–p interaction which predominantly governs the ultrasonic attenuation; outstanding to deficiency of theoretical or experimental data in the works, a comparison of UA could not be made.

From Figure 7, it is clear that the thermo-elastic loss is much small in comparison to Akhieser loss for nanostructured Cr_2N thin films. Ul-

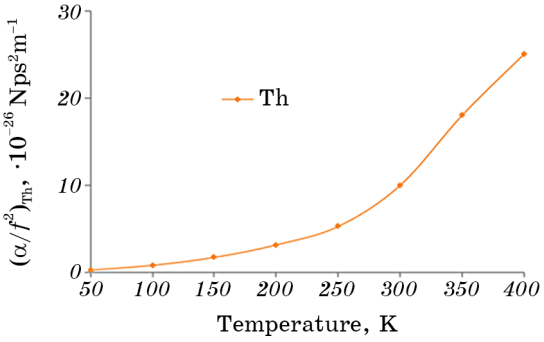

Fig. 7. $(\alpha/f^2)_{Akh}$ *vs* temperature of Cr_2N thin film.

trasonic attenuation due to p–p interaction for longitudinal wave and shear wave is leading factor. The thermal conductivity and thermal energy density are main factor that affects the total attenuation. Thus, it may be predicted that Cr_2N thin film behaves as his purest form at low temperature and are further ductile demonstrated by the minimum attenuation although at higher temperatures of Cr_2N thin film are least ductile. Therefore, at low temperature (50 K) there will be least impurity in Cr_2N thin film. The minimum UA for Cr_2N thin film minimum defends its quite stable state. Also, mechanical thins of Cr_2N thin film are superior to at low temperatures, because it has least ultrasonic attenuation and defends its rather stable hexagonal type structure state.

4. CONCLUSIONS

In conclusion, the principle established on simple interaction potential model remains valid for calculating higher-order elastic coefficients for hexagonally Cr_2N compound. It has been found that the nanostructured Cr_2N film is mechanically stable. Cr_2N compound has anisotropic structures as projected using numerous anisotropic parameters. Nanostructured Cr_2N thin film is anisotropic, which designate that the Cr–N bonds are stronger in the layer that one is parallel to the [001] plane than between the layers. The thermal relaxation time of thin film is found to be of the order of picoseconds, which defends their hexagonal structure. As τ has smallest value along $\theta = 90°$, at all temperatures, the time for re-establishment of equilibrium distribution of phonons will be minimum for the wave propagation in this direction. Over total attenuation, ultrasonic attenuation caused by p–p interaction mechanism is dominant and is a leading factor of thermal conductivity. The Cr_2N thin film behave as its purest form at low temperature and are more ductile demonstrated by the minimum attenuation while at higher temperatures Cr_2N thin are least ductile.

REFERENCES

1. S. Williams, J. L. Tipper, E. Ingham, M. H. Stone, and J. Fisher, *Proc. Inst. Mech. Eng.*, **217**: 155 (2003).
2. J. Lin, Z. L. Wu, X. H. Zhang, B. Mishra, J. J. Moore, and W. D. Sproul, *Thin Solid Films*, **517**: 1887 (2009).
3. Z. B. Qi, B. Liu, Z. T. Wu, F. P. Zhu, Z. C. Wang, and C. H. Wu, *Thin Solid Films*, **544**: 515 (2013).
4. C. A. Huang, U. W. Lieu, and C. H. Chuang, *Surf. Coat. Technol.*, **203**: 2921 (2009).
5. R. Bayyn, A. Igartua, X. Fernández, R. Martínez, R. J. Rodriguez, and J. A. García, *Analytical and Bioanalytical Chemistry*, **396**: 2855 (2009).

6. S. F. Zhu, L. Chen, Y. P. Wu, T. W. Liu, K. Tang, and Q. Wei, *Corros. Sci.*, **82**: 420 (2014).
7. P. Eklund, S. Kerdsongpanya, and B. Alling, *J. Mater. Chem. C*, **4**: 3905 (2016).
8. B. W. Karr, I. Petrov, D. G. Cahill, and J. E. Greene, *Appl. Phys. Lett.*, **70**: 1703 (1997).
9. S. Logothetidis, P. Patsalas, K. Sarakinos, C. Charitidis, and C. Metaxa, *Surf. Coat. Technol.*, **637**: 180 (2004).
10. M. Sikkens, A. M. T. Van Heereveld, E. Vogelzang, and C. A. Boose, *Thin Solid Films*, **108**: 167 (2020).
11. D. Gall, C. S. Shin, R. T. Haasch, I. Petrov, and J. E. Greene, *J. Appl. Phys.*, **91**: 5882 (2002).
12. Z. Zhou, S. Luo, Y. Wang, Z. Ai, C. Liu, and D. Wang, *Thin Solid Films*, **519**: 989 (2011).
13. P. K. Yadawa, *Pramana*, **76**, No. 4: 613 (2011).
14. D. K. Pandey, P. K. Yadawa, and R. R. Yadav, *Mater. Lett.*, **61**: 5194 (2007).
15. W. Voigt, *Lehrbuch der Kristallphysik (mit Ausschluss der Kristalloptik)* (Springer: 1966).
16. A. Reuss, *J. Applied Mathematics and Mechanics*, **9**, No. 1: 49 (1929).
17. R. Hill, *Phys. Soc. A*, **65**: 349 (1952).
18. N. Turkdal, E. Deligoz, H. Ozisik, and H. B. Ozisik, *Phase Transitions*, **90**: 598 (2017).
19. P. F. Weck, E. Kim, V. Tikare, and J. A. Mitchell, *Dalton Trans.*, **44**: 18769 (2015).
20. D. Singh, D. K. Pandey, P. K. Yadawa, and A. K. Yadav, *Cryogenics*, **49**: 12 (2009).
21. S. P. Singh, P. K. Yadawa, P. K. Dhawan, A. K. Verma, and R. R. Yadav, *Cryogenics*, **100**: 105 (2019).
22. D. Singh, P. K. Yadawa, and S. K. Sahu, *Cryogenics*, **50**: 476 (2010).
23. G. Alexander, R. A. Kvashnin, I. A. Oganov, and A. Z. Samtsevich, *J. Phys. Chem. Lett.*, **8**, No. 4: 755 (2017).
24. N. Yadav, S. P. Singh, A. K. Maddheshiya, P. K. Yadawa, and R. R. Yadav, *Phase Transitions*, **93**: 883 (2020).
25. C. P. Yadav, D. K. Pandey, and D. Singh, *Indian J. Phys.*, **93**: 1147 (2019).
26. A. F. Goncharov, M. Gauthier, D. Antonangeli, S. Ayrinhac, F. Decremps, M. Morand, A. Grechnev, S. M. Tretyak, and A. Freiman, *Phys. Rev. B*, **95**: 214104 (2017).
27. H. S. Akkera, N. N. K. Reddy, and M. C. Sekhara, *Materials Research*, **20**, No. 3: 717 (2017).
28. P. K. Yadawa, *Arabian J. Sci. Eng.*, No. 37: 255 (2012).
29. P. K. Yadawa, *Adv. Mat. Lett.*, **2**: 157 (2011).
30. J. Feng, B. Xiao, C. L. Wan, Z. X. Qu, Z. C. Huang, J. C. Chen, R. Zhou, and W. Pan, *Acta Mater.*, **59**: 1742 (2011).
31. A. K. Jaiswal, P. K. Yadawa, and R. R. Yadav, *Ultrasonics*, **89**: 22 (2018).
32. S. P. Singh, G. Singh, A. K. Verma, P. K. Yadawa, and R. R. Yadav, *Pramana*, **93**: 83 (2019).
33. P. K. Yadawa, *Ceramics-Silikáty*, **55**: 127 (2011).
34. R. I. Romanishin, I. M. Romanishin, M. M. Student, V. M. Gvozdetskii, B. P. Rusin, G. I. Romanishin, V. V. Koshevoi, S. I. Semak, and R. E. Krygul, *Russian J. Nondestructive Testing*, **55**: 479 (2018).